Copy 2
RM SE55D12

RESEARCH MEMORANDUM

for the

Bureau of Aeronautics, Department of the Navy

ALTITUDE PERFORMANCE OF MODIFIED J71 AFTERBURNER WITH REVISED ENGINE OPERATING CONDITIONS

By James W. Useller and Robert E. Russey

Lewis Flight Propulsion Laboratory
Cleveland, Ohio

NATIONAL ADVISORY COMMITTEE
FOR AERONAUTICS

WASHINGTON
May 13 1955

CONFIDENTIAL

NATIONAL ADVISORY COMMITTEE FOR AERONAUTICS

RESEARCH MEMORANDUM

for the

Bureau of Aeronautics, Department of the Navy

ALTITUDE PERFORMANCE OF MODIFIED J71 AFTERBURNER WITH REVISED ENGINE OPERATING CONDITIONS

By James W. Useller and Robert E. Russey

SUMMARY

An investigation was conducted in an altitude test chamber at the NACA Lewis laboratory to determine the effect of a revision of the rated engine operating conditions and modifications to the afterburner fuel system, flameholder, and shell cooling on the augmented performance of the J71-A-2(X-29) turbojet engine operating at altitude. The afterburner modifications were made by the manufacturer to improve the endurance at sea-level, high-pressure conditions and to reduce the afterburner shell temperatures. The engine operating conditions of rated rotational speed and turbine-outlet gas temperature were increased. Data were obtained at conditions simulating flight at a Mach number of 0.9 and at altitudes from 40,000 to 60,000 feet.

The afterburner modifications caused a reduction in afterburner combustion efficiency. The increase in rated engine speed and turbine-outlet temperature coupled with the afterburner modifications resulted in the over-all thrust of the engine and afterburner being unchanged at a given afterburner equivalence ratio, while the specific fuel consumption was increased slightly. A moderate shift in the range of equivalence ratios over which the afterburner would operate was encountered, but the maximum operable altitude remained unaltered. The afterburner-shell temperatures were also slightly reduced because of the modifications to the afterburner.

INTRODUCTION

As a part of the development program of the J71 turbojet engine, modifications were made to the afterburner fuel system, flameholder, and shell cooling configuration by the manufacturer to improve the endurance at sea-level, high-pressure conditions. The rated operating conditions

of turbine-outlet gas temperature and the rotational speed of the basic engine were increased. The effect of these modifications on the altitude performance of the engine and afterburner combination was evaluated as part of an altitude investigation of this engine being conducted by the NACA Lewis laboratory.

The investigation was conducted in an altitude test chamber at conditions simulating flight at a flight Mach number of 0.9 and at altitudes from 40,000 to 60,000 feet. The effect of the revised engine rated conditions and the afterburner modifications on the thrust, the specific fuel consumption, and the afterburner combustion performance are presented. The influence of the configuration changes on the range of operable altitudes and afterburner equivalence ratios was also determined. Data showing the distribution of the longitudinal afterburner-shell temperature are included.

APPARATUS AND PROCEDURE

Afterburner Configuration

The J71-A-2 afterburner has a nominal length of 11 feet from the turbine outlet to the exhaust-nozzle exit and a diameter of 40 inches. A schematic diagram of the afterburner showing the location of the various components is shown in figure 1. The basic configuration of the revised afterburner is similar to that of reference 1 with the following modifications:

(1) The mean height of the afterburner cooling-liner passage was increased from 0.48 to 0.93 inch, doubling the cross-sectional flow area and increasing the cooling-air-flow rate.

(2) The fuel-spray bars were redesigned to reduce the shell cooling problems during sea-level operation. The orifices of the primary fuel system were changed in diameter slightly and their radial position shifted inward from the afterburner wall. The secondary fuel system was not used in this investigation. Details of the modified spray bars are shown in figure 2.

(3) The radial gutters between the rings of the flameholder were removed to improve the endurance of the flameholder. The total blocked area of the flameholder was maintained constant by increasing the gutter width and reducing the diameter of the outer ring slightly. Flameholder dimensions are shown in figure 1, and a photograph of the flameholder is shown in figure 3.

Engine Installation

The present investigation was conducted in an altitude test chamber in which pressures and temperatures simulating altitude flight conditions were supplied to the engine inlet. Altitude pressures were simulated at the engine exhaust.

A J71-A-2(X-29) turbojet engine was used as the basic test vehicle. The engine has a bifurcated inlet, a 16-stage axial-flow compressor, and a three-stage turbine. The engine was operated at the revised rated rotational speed of 6175 rpm and a turbine-outlet gas temperature of 1700° R as measured by the manufacturer's thermocouples. The original rated conditions of this engine were a rotational speed of 6100 rpm and a turbine-outlet gas temperature of 1670° R. Although the complete engine and afterburner configuration will include an ejector for cooling the downstream end of the afterburner, the ejector was not installed during this investigation.

Fuel conforming to MIL-F-5624A grade JP-4 specifications was used in the engine and afterburner. The lower heating value of the fuel is 18,700 Btu per pound and the hydrogen-carbon ratio is 0.169.

Instrumentation

The afterburner-inlet conditions were surveyed by 25 total-pressure and 25 total-temperature probes. Data from these probes were used to calculate engine and afterburner performance. The manufacturer's thermocouples were used as sensors for the engine control system and as an indication of the turbine-outlet gas temperature. The afterburner-shell cooling-air-flow rate was measured by four total-pressure probes and a single stream static-pressure probe placed in the cooling passage. A water-cooled rake at the exhaust-nozzle inlet containing 14 total-pressure probes placed on centers of equal area provided a survey of the afterburner-outlet total pressure.

The afterburner-shell temperature was measured by single thermocouples placed longitudinally at 1-foot intervals. A circumferential temperature survey of the shell in the plane of the exhaust-nozzle inlet was made by six equally spaced thermocouples.

Standard engine instrumentation was used to measure the air flow, engine and afterburner fuel flows, and thrust. A detailed description of the engine instrumentation is contained in reference 2.

Procedure

The afterburner performance was determined at a flight Mach number of 0.9 and at altitudes of 40,000, 50,000, and 60,000 feet with the engine operating at rated rotational speed and exhaust-gas temperature. Data were obtained at each flight condition for a range of equivalence ratios (fraction of stoichiometric fuel-air ratio) from approximately 0.4 to 1.1.

In order to determine the effect of removal of the flameholder radial gutters, the afterburner was operated with both the original and modified flameholders at similar conditions. The modified fuel-spray distribution and cooling-liner geometry were used in both cases.

For the determination of the operational range of the afterburner, the limit of the lean fuel-air ratio was established by combustion blowout, while the rich limit was imposed by the maximum area of the exhaust nozzle. All data were obtained without the afterburner ejector in order to permit computation of combustion efficiency and temperature.

A list of the symbols used in this report is given in appendix A, and an explanation of the method of calculation is presented in appendix B.

DISCUSSION

The experimental data obtained in this investigation are presented in tabular form in table I, and the pertinent performance parameters are shown in figures 4 to 9. The performance of the original afterburner configuration (ref. 1) is included in these figures for comparison.

As a part of the effort to reduce the afterburner-shell temperature, the fuel-spray pattern was shifted radially away from the outer wall. The modification to the fuel pattern caused a change in the fuel-air distribution and mixing, contributing to a decrease in combustion efficiency from that of reference 1, as shown in figure 4. The greatest decrease in combustion efficiency occurred at 50,000 feet at the lower equivalence ratios. The removal of the radial gutters and the redesign of the annular rings of the flameholder to maintain the blocked area constant caused no measureable change in either combustion temperature or efficiency, as may be seen in figure 5. The modification of the cooling-liner geometry could contribute to the reduction of the combustion efficiency, although this effect has not been isolated. The flameholder changes, however, did cause an increase of approximately 1 percent in the total-pressure losses induced by the flameholder. This 1-percent change in total-pressure loss was determined by operating the modified afterburner with both the original and the revised flameholders (data not presented herein).

As a means of providing additional cooling to the afterburner structure, the cooling-air-flow rate was increased to 17 percent of the total gas flow through the afterburner (approximately three times the original flow rate). The change in geometry of the cooling passage necessary to accomodate the increased cooling-air-flow rate had little effect on the total-pressure loss through the afterburner. The over-all pressure loss in the afterburner, including both the flameholder and cooling-air-passage changes, was not significantly different from that of the original configuration of reference 1, as may be seen in figure 6. The pressure-loss data of reference 1 are shown as a shaded area because of the scatter of the data encountered. Although the scatter tends to obscure any difference in the total-pressure losses, the levels appear to be approximately the same.

The revision of the engine operating conditions of turbine-outlet temperature to 1700° R and rotational speed to 6175 rpm produced an increase in the unaugmented thrust of the engine. However, at any given equivalence ratio, the augmented thrust of the engine and afterburner was no greater than that of the original configuration because of the reduced augmentation provided by the afterburner (fig. 7(a)). The associated specific fuel consumption is shown in figure 7(b). The decreased combustion efficiency of the afterburner of this investigation is reflected in the higher specific fuel consumption.

The range of operable equivalence ratios and altitudes for the modified afterburner is shown in figure 8. The lean blow-out limit was moved to higher equivalence ratios as a result of the removal of the flameholder radial gutters. The limit of maximum-equivalence-ratio operation shown in figure 8 is limiting temperature of the turbine-outlet gas and thus is a function of the exhaust-nozzle area. The range of exhaust-nozzle areas was the same for both afterburners. The slightly higher equivalence ratio shown for the limit of the modified afterburner resulted from the lower combustion efficiency associated with this configuration. It should be noted that while the lean and rich operating limits were changed, the maximum altitude of operation was unaltered by the configuration modifications.

Some lowering of the local shell temperatures resulted from the fuel distribution modification and the increase in the cooling-air-flow rate. The temperature distribution along the afterburner length is shown in figure 9. The large reduction in shell temperatures in the location of 93 inches resulted from the large quantity of cooling air that was bled from the cooling liner into the gas stream in this region.

Lewis Flight Propulsion Laboratory
National Advisory Committee for Aeronautics
Cleveland, Ohio, May 27, 1955

APPENDIX A

SYMBOLS

The following symbols are used in this report:

$C_{v,ef}$	nozzle effective velocity coefficient
F_j	augmented jet thrust, lb
F_n	augmented net thrust, lb
f/a	fuel-air ratio
g	acceleration due to gravity, 32.17 ft/sec^2
P	total pressure, lb/sq ft abs
R	gas constant, $\frac{1546 \text{ ft-lb}}{(\text{molecular wt.})(\text{lb})(^\circ R)}$
sfc	specific fuel consumption, (lb/hr)/lb
T	total temperature, $^\circ R$
V	velocity, ft/sec
w_a	air-flow rate, lb/sec
w_f	fuel-flow rate, lb/sec
w_g	weight-flow rate, lb/sec
γ	ratio of specific heats
η	efficiency
φ	equivalence ratio

Subscripts:

ab	afterburner
ac	actual
c	cooling liner

e	engine
i	ideal
2	compressor inlet
5	turbine outlet
9	exhaust-nozzle inlet

APPENDIX B

METHOD OF CALCULATIONS

Equivalence Ratio

The afterburner equivalence ratio is defined as the fraction of stoichiometric fuel-air ratio in the afterburner

$$\varphi = \frac{(f/a)_{ab}}{0.0674}$$

where 0.0674 is the stoichiometric fuel-air ratio for the fuel used in this investigation. The afterburner fuel-air ratio is defined as follows:

$$(f/a)_{ab} = \frac{w_{f,ab} + w_{f,e} - w_{f,e,i}}{w_{a,5} - \frac{w_{f,e,i}}{0.0674}}$$

where $w_{f,e,i}$ is the fuel flow required to obtain the actual temperature rise from station 2 to station 5 with ideal efficiency. The afterburner fuel-air ratio is based on the total air flow through the afterburner including the cooling air supplied to the liner. The cooling-air flow is bled into the afterburner gas stream.

Over-All Specific Fuel Consumption

The over-all specific fuel consumption is based on the augmented net thrust and the sum of the engine and afterburner fuel flows.

Combustion Efficiency

The combustion efficiency of the afterburner was determined as a ratio of the actual to the ideal temperature rise across the afterburner. The actual combustion temperature T_9 was calculated from the gas-flow rate, the measured thrust, and a pressure survey at station 9 by using the jet-thrust equation as follows:

$$T_9 = \left[\left(\frac{F_j}{w_{g,9}}\right)\left(\frac{g}{C_{v,ef}\sqrt{gR}}\right)\left(\frac{\sqrt{gRT}}{V}\right)\right]^2$$

Values of the effective velocity parameter $\frac{V}{\sqrt{gRT}}$ were obtained from reference 3 with appropriate values for γ_9. The combustion-efficiency defining equation is as follows:

$$\eta_{ab} = \frac{[\Delta T]_{5,ac}^{9}}{[\Delta T]_{5,i}^{9}}$$

where the ideal temperature rise was determined from unpublished data.

REFERENCES

1. Useller, James W., and Mallett, William E.: Preliminary Altitude Performance Data of J71-A2 Turbojet Engine Afterburner. NACA RM SE54J06, 1954.

2. Useller, James W., and Mallett, William E.: Preliminary Altitude Performance Data for the J71-A2 (X-26) Turbojet Engine. NACA RM SE54H06, 1954.

3. Turner, L. Richard, Addie, Albert N., and Zimmerman, Richard H.: Charts for the Analysis of One-Dimensional Steady Compressible Flow. NACA TN 1419, 1948.

TABLE I. - MODIFIED J71-A-2(X-29) TURBOJET-ENGINE AFTERBURNER PERFORMANCE DATA

[Flight Mach number, 0.9]

Run	Altitude, ft	Afterburner equivalence ratio, ϕ	Compressor			Engine fuel flow, $W_{f,e}$, lb/hr	Afterburner						Jet thrust, F_j, lb	Net thrust, F_n, lb	Ratio of cooling-liner flow to gas flow, $\frac{W_{g,c}}{W_{g,5}}$
			Inlet total pressure, P_2, $\frac{lb}{sq\ ft\ abs}$	Inlet total temperature, T_2, $^\circ R$	Inlet air flow, W_a, lb/sec		Fuel flow, $W_{f,ab}$, lb/hr	Inlet gas flow, $W_{g,5}$, lb/sec	Inlet total pressure, P_5, $\frac{lb}{sq\ ft\ abs}$	Inlet total temperature, T_5, $^\circ R$	Outlet total temperature, T_9, $^\circ R$	Total-pressure loss, $\frac{P_5 - P_9}{P_5}$			
Original flameholder configuration															
1	50,000	0	401	454	33.65	2050	0	33.64	1015	1648	----	0.0631	2608	1696	0.1352
2		.484	399	452	33.62	2029	2,778	32.79	987	1652	2824	.0871	3373	2464	.1560
3		.539	401	450	33.84	2045	3,120	33.02	985	1652	2920	.0894	3459	2546	.1586
4		.634	403	450	33.87	2034	3,691	33.05	989	1652	3068	.0920	3564	2650	.1598
5		.688	402	448	34.02	2045	4,033	33.20	990	1653	3149	.0939	3635	2711	.1610
6		.759	400	448	33.92	2040	4,442	33.11	986	1653	3235	.0964	3688	2775	.1610
7	60,000	0	250	450	20.96	1309	0	20.96	608	1648	----	0.0757	1587	1021	0.1502
8		.516	248	452	20.83	1299	1,829	20.64	603	1648	2779	.0979	2051	1488	.1647
9		.557	253	450	21.00	1299	2,010	20.81	602	1648	2863	.1013	2099	1533	.1645
10		.646	249	448	20.93	1290	2,345	20.74	601	1648	3026	.1032	2172	1608	.1661
11		.699	245	456	20.74	1290	2,492	20.47	599	1648	3063	.1052	2175	1613	.1694
12		.734	245	446	21.09	1309	2,673	20.89	605	1648	3160	.1058	2258	1691	.1673
Modified flameholder configuration															
13	40,000	0	651	451	54.09	3275	0	55.00	1701	1658	----	0.0602	4293	2809	0.1096
14		.457	651	456	54.70	3230	4,344	53.42	1642	1656	2802	.0802	5507	4021	.1384
15		.534	660	454	55.49	3280	5,142	54.16	1644	1657	3018	.0846	5797	4293	.1433
16		.743	659	453	55.50	3270	7,190	54.18	1637	1659	3362	.0923	6167	4665	.1486
17		.917	662	453	55.54	3290	8,850	54.19	1640	1657	3492	.0957	6340	4837	.1498
18		.996	665	454	55.74	3315	9,628	54.36	1659	1661	3578	.0965	6477	4967	.1519
19		1.111	661	448	55.98	3290	10,841	54.60	1649	1662	3575	.0989	6530	5023	.1515
20	50,000	0	410	454	34.18	2045	0	34.08	1011	1660	----	0.0692	2627	1701	0.1370
21		.373	405	454	33.94	2045	2,178	33.18	980	1660	2450	.0837	3120	2200	.1528
22		.410	402	454	33.88	2034	2,412	33.18	989	1660	2580	.0860	3239	2319	.1543
23		.435	405	453	33.99	2034	2,546	33.19	991	1664	2694	.0878	3312	2392	.1570
24		.483	402	454	33.94	2029	2,834	33.18	983	1660	2780	.0916	3387	2467	.1585
25		.635	403	454	33.85	2030	3,725	33.18	978	1660	3070	.0982	3570	2650	.1624
26		.719	406	454	34.00	2034	4,221	33.19	981	1656	3206	.0999	3650	2729	.1636
27		.813	408	454	34.05	2018	4,798	33.22	983	1653	3305	.1028	3725	2802	.1647
28		.886	404	453	34.01	2018	5,234	33.21	973	1651	3415	.1059	3793	2872	.1653
29		.897	408	455	34.07	2024	5,287	33.24	984	1656	3418	.1057	3801	2877	.1661
30		1.024	396	449	33.63	2061	5,923	32.84	989	1667	3546	.1052	3888	2982	.1645
31	60,000	0	250	455	20.85	1295	0	20.68	607	1655	----	0.0807	1606	1040	0.1552
32		.535	250	456	20.81	1300	1,886	20.54	598	1655	2873	.1020	2058	1493	.1631
33		.570	249	455	20.69	1300	2,013	20.50	603	1655	2831	.1028	2069	1508	.1654
34		.717	249	455	20.71	1300	2,550	20.50	596	1653	3176	.1107	2199	1637	.1673
35		.845	250	456	20.79	1285	3,060	20.61	595	1647	3284	.1177	2251	1686	.1728

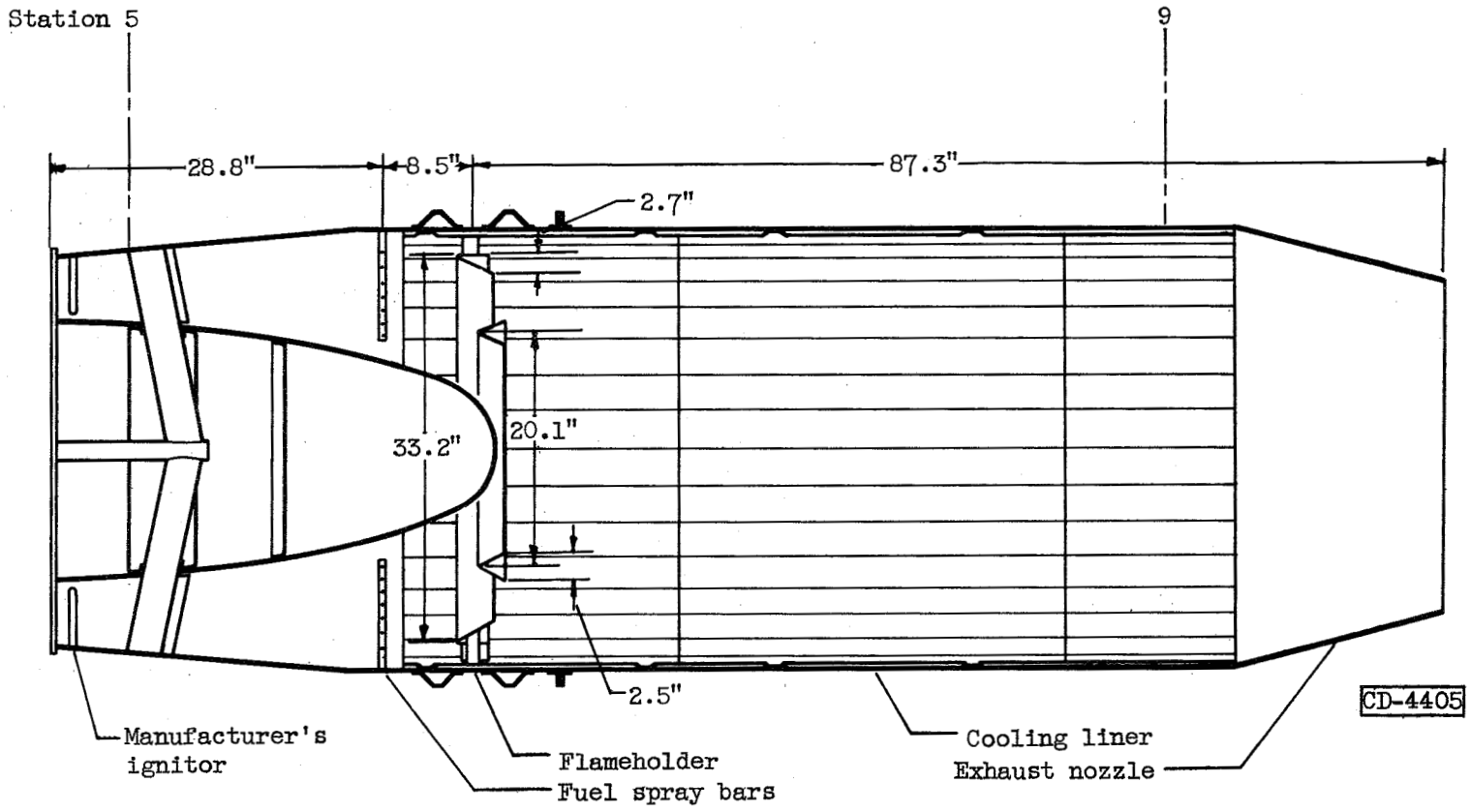

Figure 1. - Schematic diagram of J71-A-2 turbojet-engine afterburner showing location of various components.

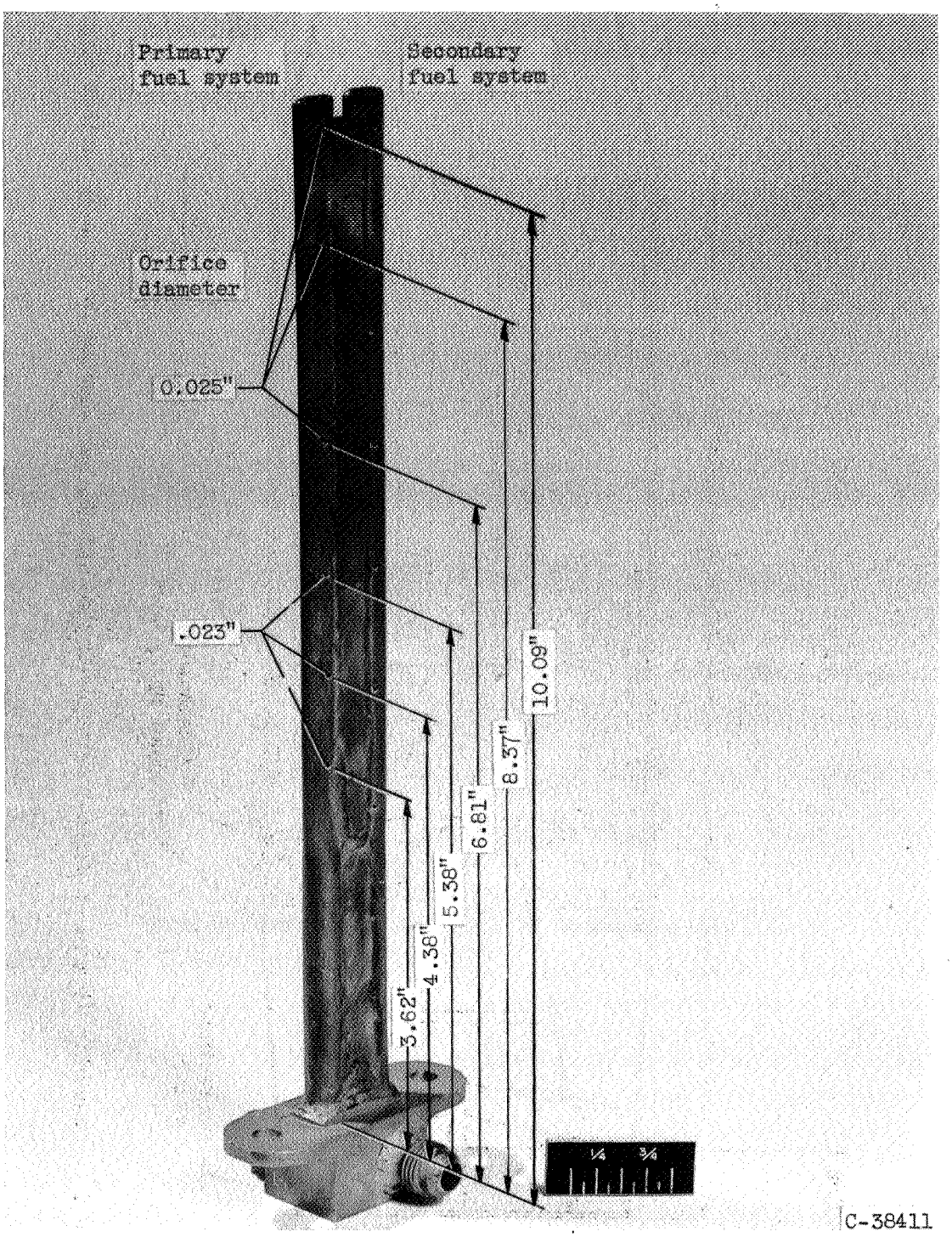

Figure 2. - J71-A-2 turbojet afterburner fuel-spray-bar details.

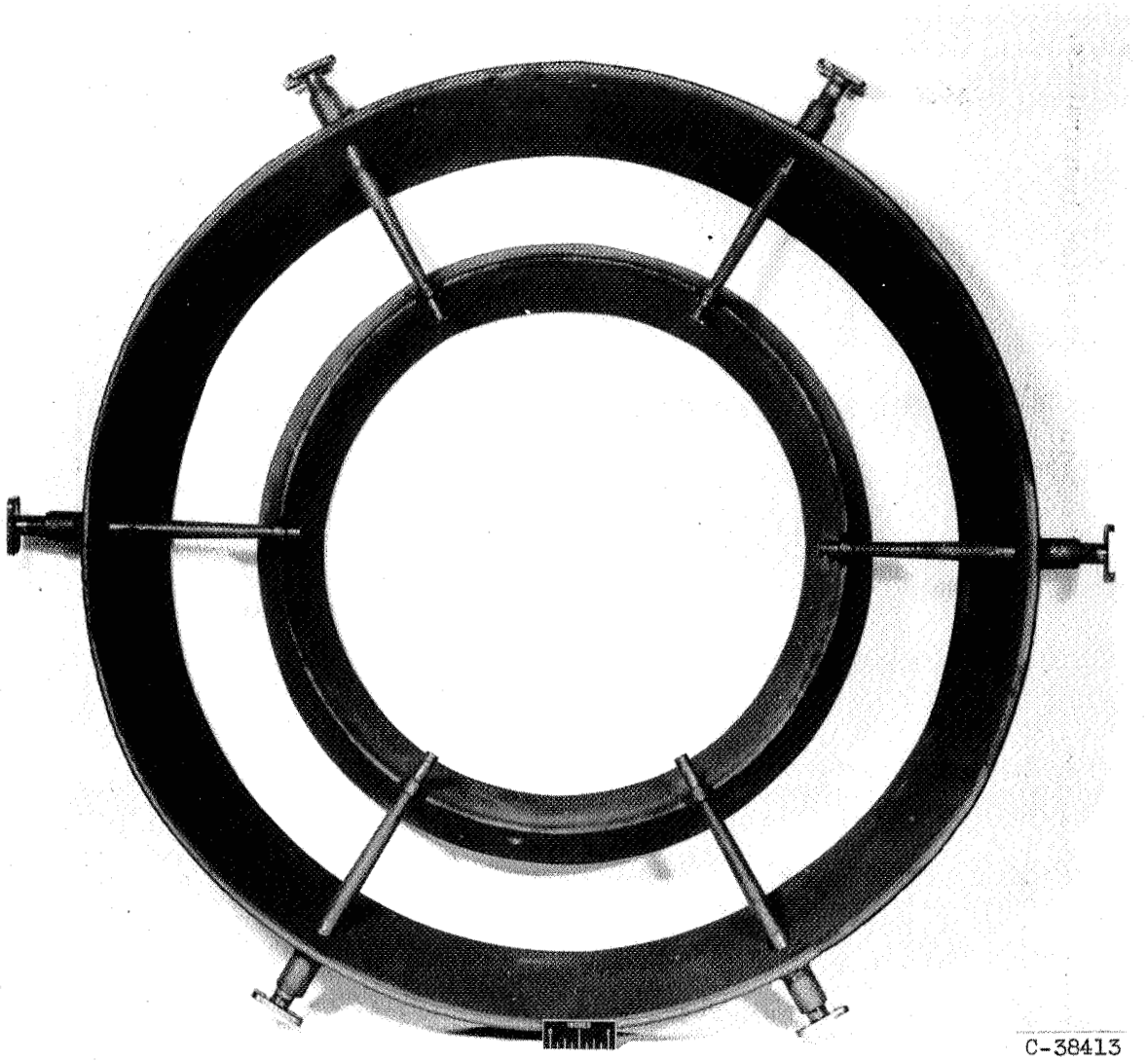

Figure 3. - J71-A-2 turbojet-engine afterburner modified flameholder.

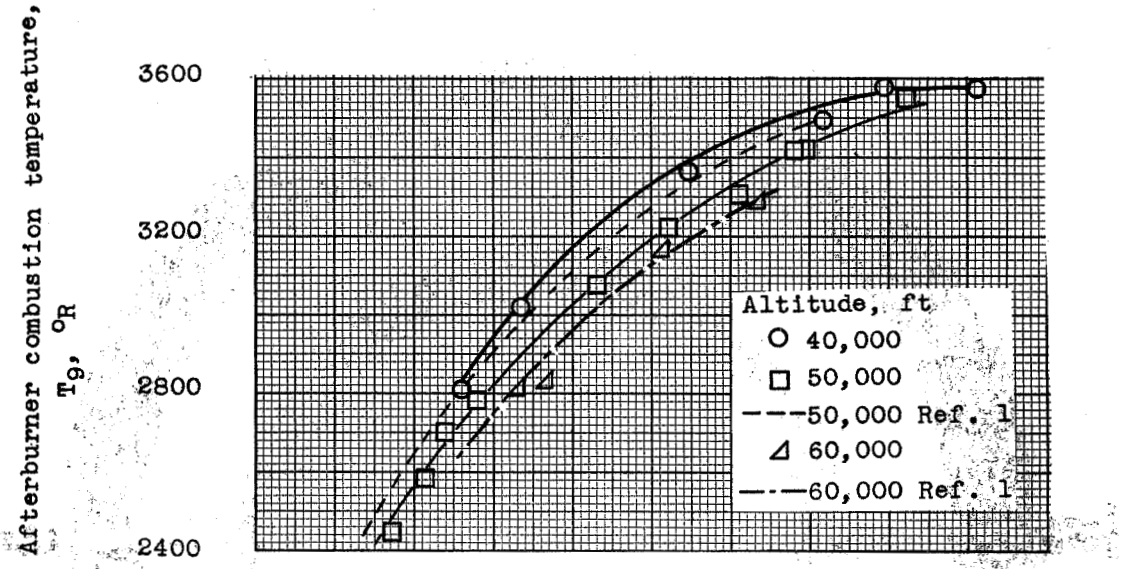

(a) Combustion temperature.

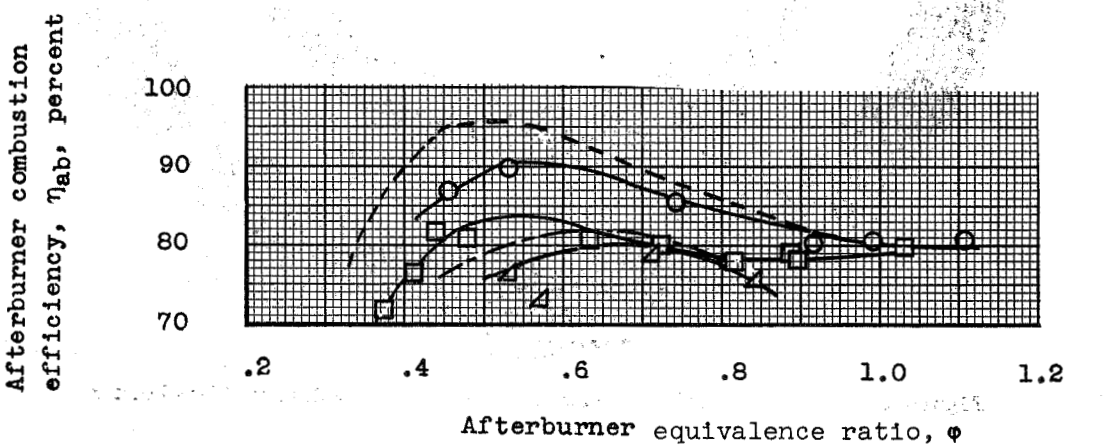

(b) Combustion efficiency.

Figure 4. - Modified J71-A-2 turbojet-engine afterburner combustion performance variation with altitude. Flight Mach number, 0.9.

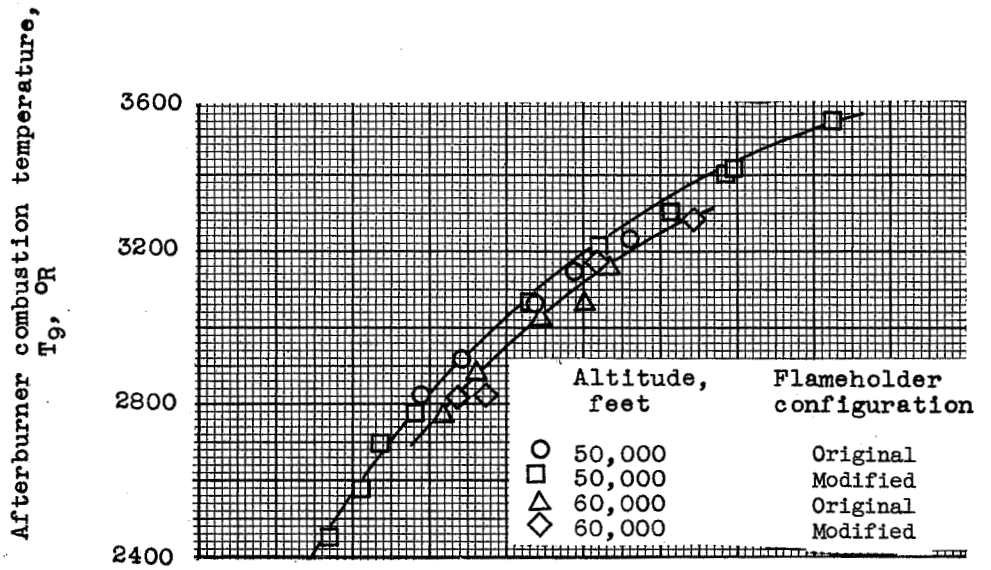

(a) Combustion temperature.

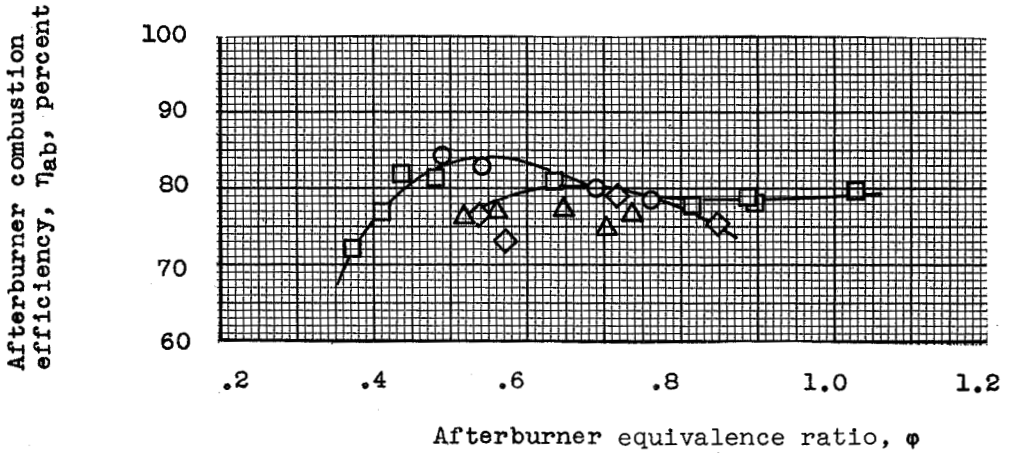

(b) Combustion efficiency.

Figure 5. - Combustion performance of modified J71-A-2 turbojet-engine afterburner with original and modified flameholders. Flight Mach number, 0.9.

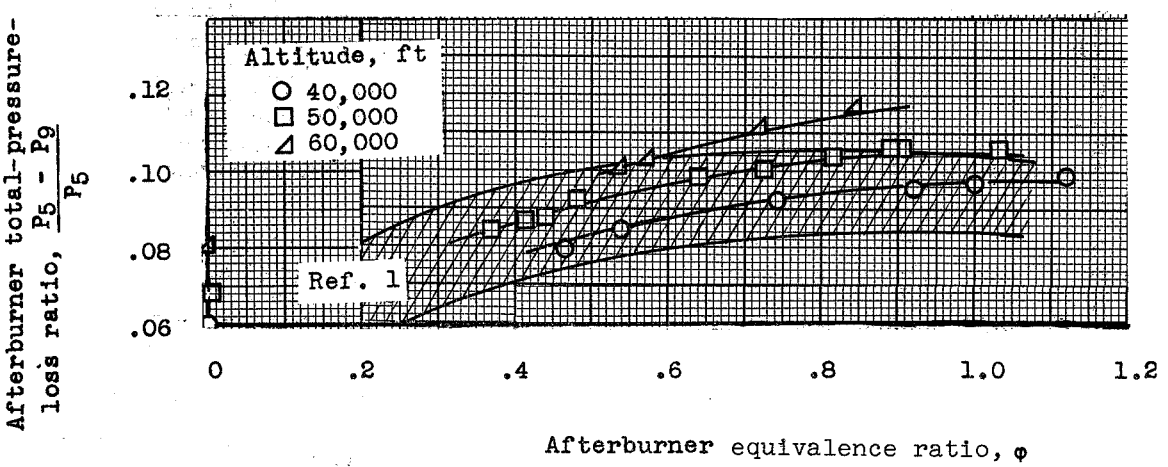

Figure 6. - Modified J71-A-2 turbojet-engine afterburner total-pressure-loss variation with altitude. Flight Mach number, 0.9.

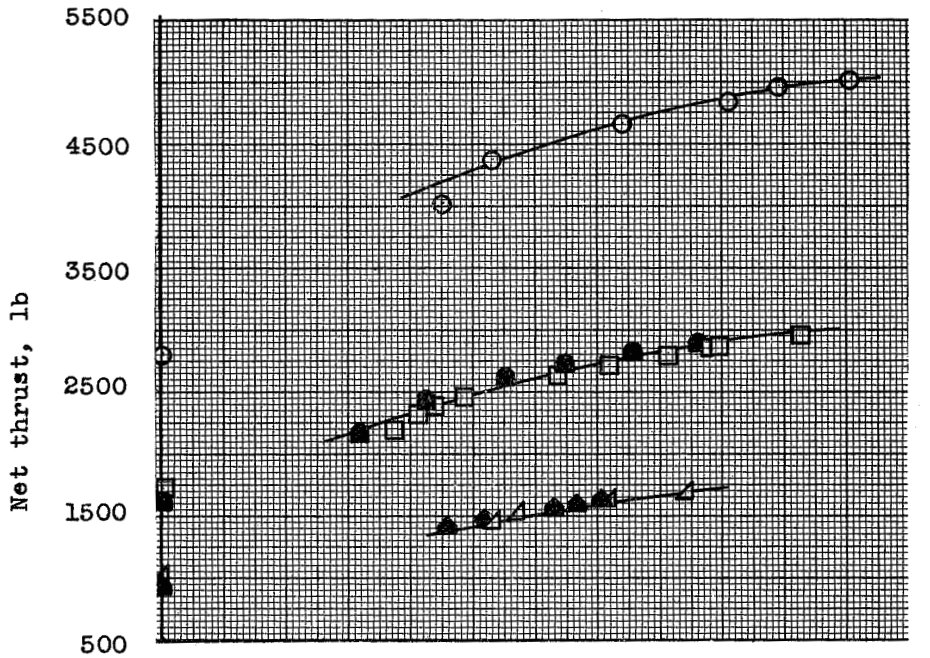

(a) Net thrust

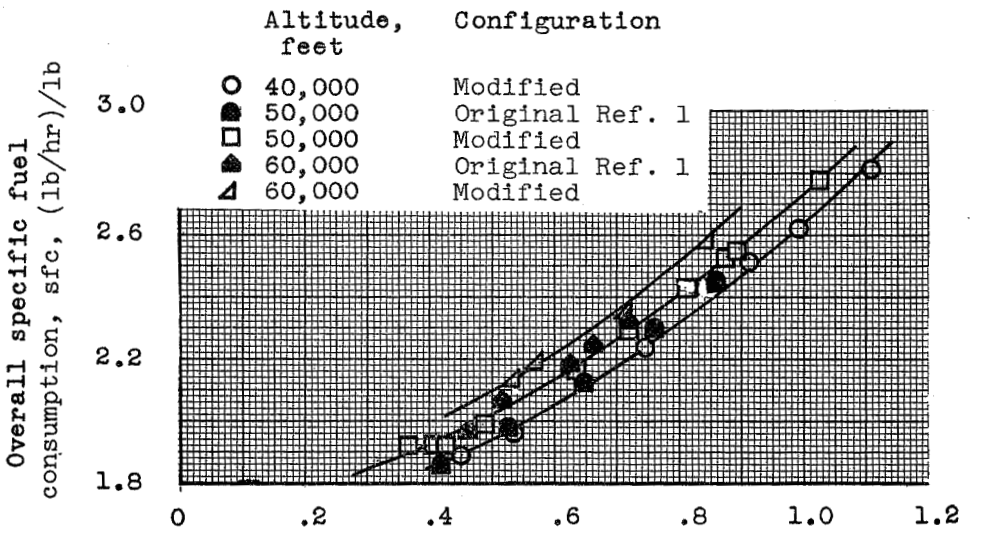

(b) Overall specific fuel consumption.

Figure 7. Performance of combined J71-A-2 turbojet engine and afterburner at altitude. Flight Mach number, 0.9.

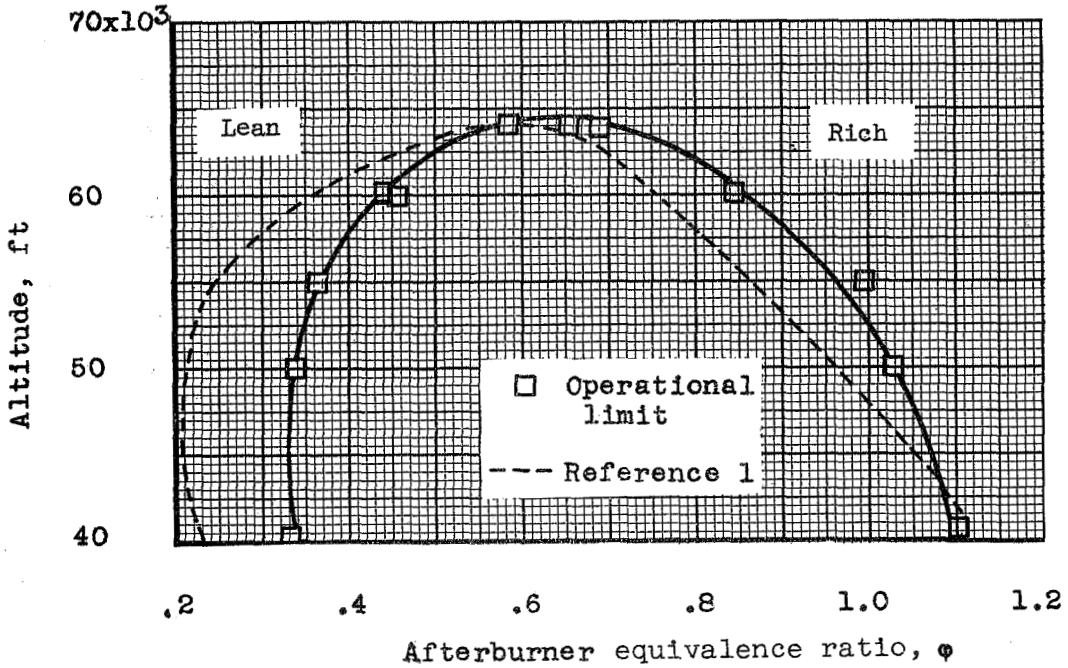

Figure 8.- Modified J71-A-2 turbojet-engine afterburner operational limits. Flight Mach number, 0.9.

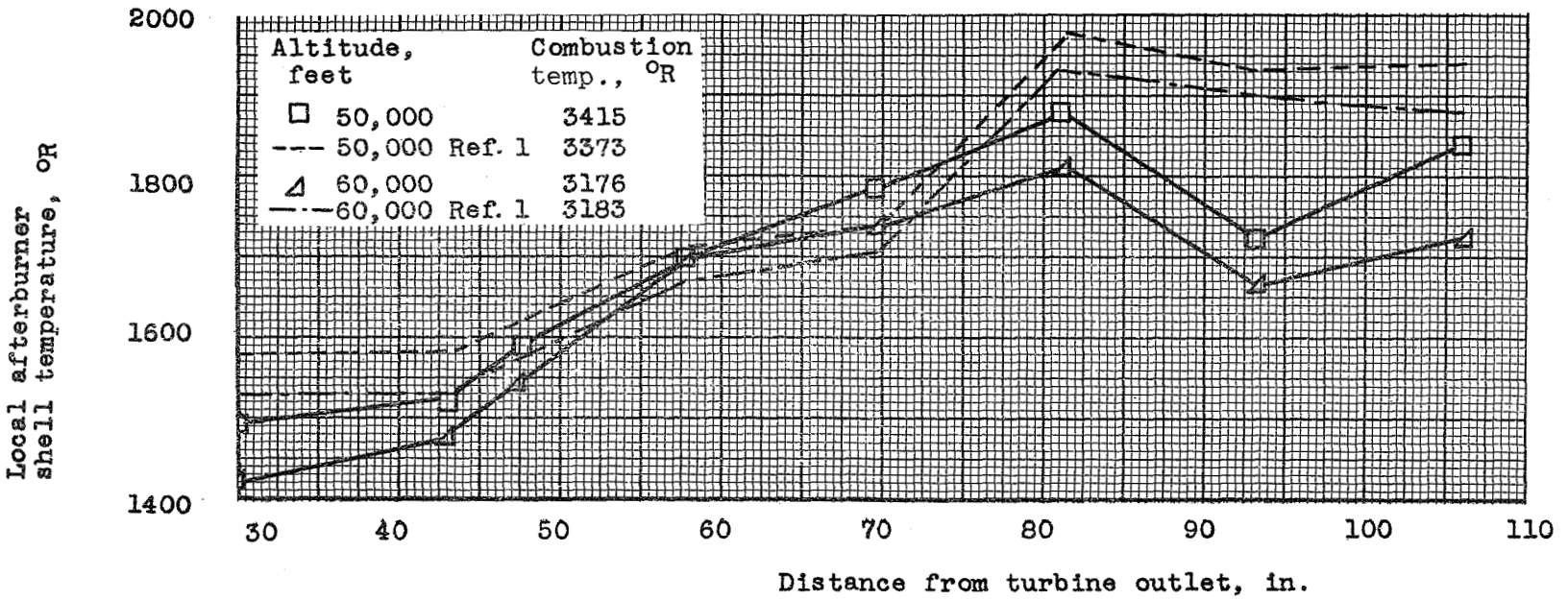

Figure 9. - Local afterburner-shell temperature distribution along length of modified J71-A2 turbojet-engine afterburner.

ALTITUDE PERFORMANCE OF MODIFIED J71 AFTERBURNER WITH REVISED ENGINE OPERATING CONDITIONS

James W. Useller
Aeronautical Research Scientist
Propulsion Systems

Robert E. Russey
Aeronautical Research Scientist
Propulsion Systems

Approved:

William A. Fleming
Aeronautical Research Scientist
Propulsion Systems

Bruce T. Lundin
Chief
Engine Research Division

cak - 5/31/55